

SEMILEPTONIC B MESON DECAYS AND THE DETERMINATION OF V_{cb} AND V_{ub}

Updated February 2014 by R. Kowalewski (Univ. of Victoria, Canada) and T. Mannel (Univ. of Siegen, Germany)

INTRODUCTION

Semileptonic B meson decay amplitudes allow determinations of $|V_{ub}|$ and $|V_{cb}|$ which are assumed to be largely free from any impact of non-standard model physics, since they are dominated by the standard-model W boson exchange. A charged Higgs boson, present in many models of new physics, will couple to the mass of the lepton and hence it will have practically no impact in decays into e and μ . However, decays to tau leptons, which are also discussed in this review, provide sensitivity to these models.

Precision determinations of $|V_{ub}|$ and $|V_{cb}|$ are central to testing the CKM sector of the Standard Model, and complement the measurements of CP asymmetries in B decays. The length of the side of the unitarity triangle opposite the well-measured angle β is proportional to the ratio $|V_{ub}|/|V_{cb}|$, making its determination a high priority of the heavy-flavor physics program.

The semileptonic transitions $b \rightarrow c\ell\bar{\nu}_\ell$ and $b \rightarrow u\ell\bar{\nu}_\ell$ (where ℓ refers to an electron or muon) each provide two avenues for determining these CKM matrix elements, namely through inclusive and exclusive final states. Recent measurements and calculations are reflected in the values quoted in this article, which is an update of the previous review [1]. The leptonic decay $B^- \rightarrow \tau\bar{\nu}$ can also be used to extract $|V_{ub}|$; we do not use this information at present since none of the current experimental measurements has reached the significance level of an observation.

The theory underlying the determination of $|V_{qb}|$ is mature, in particular for $|V_{cb}|$. Most of the theoretical approaches use the fact that the mass m_b of the b quark is large compared to the scale Λ_{QCD} that determines low-energy hadronic physics. The basis for precise calculations is a systematic expansion in powers of Λ/m_b , where $\Lambda \sim 500 - 700$ MeV is a hadronic scale

of the order of Λ_{QCD} , based on effective-field-theory methods described in a separate RPP mini-review.

The large data samples available at the B factories enable analyses where one B meson from an $\Upsilon(4S)$ decay is fully reconstructed, allowing a recoiling semileptonic B decay to be studied with high purity. Improved knowledge of $\overline{B} \rightarrow X_c \ell \overline{\nu}_\ell$ decays allows partial rates for $\overline{B} \rightarrow X_u \ell \overline{\nu}_\ell$ transitions to be measured in regions previously considered inaccessible, increasing the acceptance for $\overline{B} \rightarrow X_u \ell \overline{\nu}_\ell$ transitions and reducing theoretical uncertainties.

Experimental measurements of the exclusive $\overline{B} \rightarrow \pi \ell \overline{\nu}_\ell$ decay are quite precise, and recent improvements in the theoretical calculation of the form factor normalization have enabled a determination of $|V_{ub}|$ from this decay with an uncertainty below 10%.

The decays $\overline{B} \rightarrow D^{(*)} \tau \overline{\nu}_\ell$ provide sensitivity to possible non-universalities in the couplings to the third generation leptons that are present at tree level in models involving new charged mediators. The constraints on these models are weak at present, and the enhanced decay rates seen in recent measurements of these decay modes, if they turn out to be robust, are an indication of new physics.

Throughout this review the numerical results quoted are based on the methods of the Heavy Flavor Averaging Group [2].

DETERMINATION OF $|V_{cb}|$

Summary: The determination of $|V_{cb}|$ from $\overline{B} \rightarrow D^* \ell \overline{\nu}_\ell$ decays has a relative precision of about 2%, with the main uncertainty coming from knowledge of the form factor near the maximum momentum transfer to the leptons. The $\overline{B} \rightarrow D \ell \overline{\nu}_\ell$ decay provides a determination with an uncertainty of 5%.

Inclusive decays provide a determination of $|V_{cb}|$ with a relative uncertainty of about 2%. The limitations arise mainly from our ignorance of higher-order perturbative and non-perturbative corrections.

The values obtained from inclusive and exclusive determinations are marginally consistent with each other:

$$|V_{cb}| = (42.2 \pm 0.7) \times 10^{-3} \text{ (inclusive)} \quad (1)$$

$$|V_{cb}| = (39.5 \pm 0.8) \times 10^{-3} \text{ (exclusive);} \quad (2)$$

as a result, their combination should be treated with caution. An average of these determinations has $p(\chi^2) = 0.01$, so we scale the error by $\sqrt{\chi^2/1} = 2.6$ to find

$$|V_{cb}| = (41.1 \pm 1.3) \times 10^{-3} . \quad (3)$$

$|V_{cb}|$ from exclusive decays

Exclusive determinations of $|V_{cb}|$ are based on a study of semileptonic B decays into the ground state charmed mesons D and D^* . The main uncertainties in this approach stem from our ignorance of the form factors describing the $B \rightarrow D$ and $B \rightarrow D^*$ transitions. However, in the limit of infinite bottom and charm quark masses only a single form factor appears, the Isgur-Wise function [3], which depends on the product of the four-velocities v and v' of the initial and final-state hadrons.

The extraction of $|V_{cb}|$ is based on the distribution of the variable $w \equiv v \cdot v'$, which corresponds to the energy of the final state $D^{(*)}$ meson in the rest frame of the decay. Heavy Quark Symmetry (HQS) [3,4] predicts the normalization of the rate at $w = 1$, the point of maximum momentum transfer to the leptons, and $|V_{cb}|$ is obtained from an extrapolation of the measured spectrum to $w = 1$. This extrapolation relies on a parametrization of the form factor, as explained below.

A precise determination requires corrections to the HQS prediction for the normalization as well as some information on the slope of the form factors near the point $w = 1$. The framework for this is ‘‘Heavy Quark Effective Theory’’, which is discussed in a separate mini-review. The corrections to the HQS prediction are due to finite quark masses and are essentially of the order Λ_{QCD}/m_c . Form factors that are normalized due to HQS are protected against linear corrections of this order and hence the corrections are here of order $\Lambda_{\text{QCD}}^2/m_c^2$ due to Luke’s Theorem [5], which is an application of the Ademollo-Gatto

theorem [6] to heavy quarks. For the form factors that vanish in the infinite mass limit the corrections are in general linear in Λ_{QCD}/m_c , and thus we have, using the definitions as in Eq. (2.84) of Ref. 7

$$\begin{aligned} h_i(1) &= 1 + \mathcal{O}(\Lambda_{\text{QCD}}^2/m_c^2) && \text{for } i = +, V, A_1, A_3, \\ h_i(1) &= \mathcal{O}(\Lambda_{\text{QCD}}/m_c) && \text{for } i = -, A_2. \end{aligned} \quad (4)$$

In addition to these corrections, there are perturbatively calculable radiative corrections from hard gluons and photons, which will be discussed in the relevant sections.

$\overline{B} \rightarrow D^* \ell \overline{\nu}_\ell$

The decay rate for $\overline{B} \rightarrow D^* \ell \overline{\nu}_\ell$ is given by

$$\frac{d\Gamma}{dw}(\overline{B} \rightarrow D^* \ell \overline{\nu}_\ell) = \frac{G_F^2 m_B^5}{48\pi^3} |V_{cb}|^2 (w^2 - 1)^{1/2} P(w) (\eta_{\text{ew}} \mathcal{F}(w))^2, \quad (5)$$

where $P(w)$ is a phase space factor,

$$P(w) = r^3 (1 - r)^2 (w + 1)^2 \left(1 + \frac{4w}{w + 1} \frac{1 - 2rw + r^2}{(1 - r)^2} \right).$$

with $r = m_{D^*}/m_B$. The form factor $\mathcal{F}(w)$ is dominated by the axial vector form factor h_{A_1} as $w \rightarrow 1$. Furthermore, $\eta_{\text{ew}} = 1.007$ accounts for the electroweak corrections to the four-fermion operator mediating the semileptonic decay [8]. In the infinite-mass limit, the HQS normalization gives $\mathcal{F}(1) = 1$.

The form factor $\mathcal{F}(w)$ must be parametrized to perform an extrapolation to the zero-recoil point. A frequently used one-parameter form motivated by analyticity and unitarity is [9,10]

$$\begin{aligned} h_{A_1}(w) &= \eta_A \left[1 + \delta_{1/m^2} + \dots \right] \\ & \left[1 - 8\rho_{A_1}^2 z + (53\rho_{A_1}^2 - 15)z^2 - (231\rho_{A_1}^2 - 91)z^3 \right] \end{aligned} \quad (6)$$

with $z = (\sqrt{w + 1} - \sqrt{2})/(\sqrt{w + 1} + \sqrt{2})$ originating from a conformal transformation. The parameter $\rho_{A_1}^2$ is the slope of the form factor at $w = 1$. The factor η_A is the QCD short-distance radiative correction [11] to the form factor

$$\eta_A = 0.960 \pm 0.007, \quad (7)$$

and δ_{1/m^2} comes from non-perturbative $1/m^2$ corrections.

Precise lattice determinations of the $B \rightarrow D^{(*)}$ form factors naturally build in heavy-quark symmetries, so all uncertainties scale with the deviation of the form factor from unity. Unquenched calculations, i.e. calculations with realistic sea quarks, obtain quite precise predictions of the form factors; the relevant calculations for the form factor $\mathcal{F}(\omega)$ in Refs. [12,13] quote a total uncertainty at the 2% level. The main contributions to this uncertainty are from the chiral extrapolation from the light quark masses used in the numerical lattice computation to realistic up and down quark masses, and from discretization errors. These sources of uncertainty will be reduced with larger lattice sizes and smaller lattice spacings.

Including effects from finite quark masses to calculate the deviation of $\mathcal{F}(1)$ from unity, the current lattice prediction is

$$\mathcal{F}(1) = 0.902 \pm 0.017, \quad (8)$$

where the factor η_{ew} has been divided out from the value quoted in Ref. 14 and the errors have been added in quadrature. The leading uncertainties are due to heavy-quark discretization and chiral extrapolation errors.

Non-lattice estimates based on sum rules for the form factor tend to yield lower values for $\mathcal{F}(1)$ [15,16,17]. Omitting the contributions from excited states, the sum rules indicate that $\mathcal{F}(1) < 0.93$. Including an estimate for the contribution of the excited states yields $\mathcal{F}(1) = 0.86 \pm 0.01 \pm 0.02$ [17,18] where the second uncertainty originates from the estimate for the excited states.

Many experiments [19–27] have measured the differential rate as a function of w . These measurements are input to a four-dimensional fit [28] for $\mathcal{F}(1)|V_{cb}|$, $\rho_{A_1}^2$ and the form factor ratios $R_1 \propto A_2/A_1$ and $R_2 \propto V/A_1$. The leading sources of uncertainty on $\mathcal{F}(1)|V_{cb}|$ are due to detection efficiencies and $D^{(*)}$ decay branching fractions, while for $\rho_{A_1}^2$ the uncertainties in R_1 and R_2 still dominate. Recent BABAR measurements, one using $\overline{B}^0 \rightarrow D^{*0} \ell \overline{\nu}_\ell$ decays [25] and the other using a global fit to $\overline{B} \rightarrow D \ell \overline{\nu}_\ell X$ decays [26] are completely insensitive to uncertainties related to the reconstruction of the charged pion

from $D^* \rightarrow D\pi$ decays; both measurements agree with the average given below.

The fit gives [29] $\eta_{\text{ew}}\mathcal{F}(1)|V_{cb}| = (35.85 \pm 0.45) \times 10^{-3}$ with a p -value of 0.15. Along with the lattice value given above for $\mathcal{F}(1)$ this yields

$$|V_{cb}| = (39.48 \pm 0.50_{\text{exp}} \pm 0.74_{\text{theo}}) \times 10^{-3} (\overline{B} \rightarrow D^* \ell \bar{\nu}_\ell, \text{LQCD}). \quad (9)$$

The value of $\mathcal{F}(1)$ obtained from QCD sum rules results in a larger value for $|V_{cb}|$:

$$|V_{cb}| = (41.4 \pm 0.5_{\text{exp}} \pm 1.0_{\text{theo}}) \times 10^{-3} (\overline{B} \rightarrow D^* \ell \bar{\nu}_\ell, \text{SR}). \quad (10)$$

$\overline{B} \rightarrow D\ell\bar{\nu}_\ell$

The differential rate for $\overline{B} \rightarrow D\ell\bar{\nu}_\ell$ is given by

$$\begin{aligned} \frac{d\Gamma}{dw}(\overline{B} \rightarrow D\ell\bar{\nu}_\ell) = \\ \frac{G_F^2}{48\pi^3} |V_{cb}|^2 (m_B + m_D)^2 m_D^3 (w^2 - 1)^{3/2} (\eta_{\text{ew}}\mathcal{G}(w))^2. \end{aligned} \quad (11)$$

The form factor is

$$\mathcal{G}(w) = h_+(w) - \frac{m_B - m_D}{m_B + m_D} h_-(w), \quad (12)$$

where h_+ is normalized to unity in the infinite-mass limit due to HQS and h_- vanishes in the heavy-mass limit. Thus

$$\mathcal{G}(1) = 1 + \mathcal{O}\left(\frac{m_B - m_D}{m_B + m_D} \frac{\Lambda_{\text{QCD}}}{m_c}\right) \quad (13)$$

and the corrections to the HQET predictions are parametrically larger than was the case for $\overline{B} \rightarrow D^* \ell \bar{\nu}_\ell$.

In order to get a more precise prediction for the form factor $\mathcal{G}(1)$ the heavy-quark expansion can be supplemented by additional assumptions. It has been argued in Ref. 30 that in a limit in which the kinetic energy μ_π^2 is equal to the chromomagnetic moment μ_G^2 (these quantities are discussed below in more detail) one may obtain the value

$$\mathcal{G}(1) = 1.04 \pm 0.01_{\text{power}} \pm 0.01_{\text{pert}}. \quad (14)$$

Lattice calculations including effects beyond the heavy mass limit have become available, and hence the fact that deviations

from the HQET predictions are parametrically larger than in the case $\overline{B} \rightarrow D^* \ell \overline{\nu}_\ell$ is irrelevant. These unquenched calculations quote a value (preliminary, from 2005) [31]

$$\mathcal{G}(1) = 1.074 \pm 0.018 \pm 0.016. \quad (15)$$

Recent, yet unpublished results indicate that the updated lattice value for $\mathcal{G}(1)$ will become slightly smaller, making it better compatible with Eq. (14).

Recent measurements of $\overline{B} \rightarrow D \ell \overline{\nu}_\ell$ [26,32] are consistent with earlier measurements [19,33,34] but are significantly more precise. The average of these inputs [29] gives $\eta_{\text{ew}} \mathcal{G}(1) |V_{cb}| = (42.5 \pm 1.6) \times 10^{-3}$. Using the value from Eq. (15) for $\mathcal{G}(1)$, accounting for the electroweak correction and conservatively adding the theory uncertainties linearly gives

$$|V_{cb}| = (39.3 \pm 1.4 \pm 1.3) \times 10^{-3} \quad (\overline{B} \rightarrow D \ell \overline{\nu}_\ell, \text{ LQCD}), \quad (16)$$

where the first uncertainty is from experiment and the second from theory.

Using the non-lattice estimate from Eq. (14) one finds $|V_{cb}| = (40.6 \pm 1.5 \pm 0.8) \times 10^{-3}$.

Measuring the differential rate at $w = 1$ is more difficult in $\overline{B} \rightarrow D \ell \overline{\nu}_\ell$ decays than in $\overline{B} \rightarrow D^* \ell \overline{\nu}_\ell$ decays, since the rate is smaller and the background from mis-reconstructed $\overline{B} \rightarrow D^* \ell \overline{\nu}_\ell$ decays is significant; this is reflected in the larger experimental uncertainty. The B factories study decays recoiling against fully reconstructed B mesons or perform a global fit to $\overline{B} \rightarrow D(X) \ell \nu$ decays. Theoretical input on the shape of the w spectrum in $\overline{B} \rightarrow D \ell \overline{\nu}_\ell$ is valuable, as precise measurements of the total rate are easier; recent measurements [26,32] of $\mathcal{B}(\overline{B} \rightarrow D \ell \overline{\nu}_\ell)$ have uncertainties of $\sim 5\%$.

The determinations from $\overline{B} \rightarrow D^* \ell \overline{\nu}_\ell$ and $\overline{B} \rightarrow D \ell \overline{\nu}_\ell$ decays are consistent, and their uncertainties are largely uncorrelated. Averaging the two lattice-based results quoted above gives

$$|V_{cb}| = (39.5 \pm 0.8) \times 10^{-3} \quad (\text{exclusive}). \quad (17)$$

$|V_{cb}|$ from inclusive decays

At present the most precise determination of $|V_{cb}|$ comes from inclusive decays. The method is based on a measurement of the total semileptonic decay rate, together with the leptonic energy and the hadronic invariant mass spectra of inclusive semileptonic decays. The total decay rate can be calculated quite reliably in terms of non-perturbative parameters that can be extracted from the information contained in the spectra.

Inclusive semileptonic rate

The theoretical foundation for the calculation of the total semileptonic rate is the Operator Product Expansion (OPE) which yields the Heavy Quark Expansion (HQE) [35,36]. Details of this can be found in the separate mini-review on Effective Theories. The validity of the OPE is proven in the deep Euclidean region for the momenta (which is satisfied, *e.g.*, in deep inelastic scattering), but its application to heavy-quark decays requires a continuation to time-like momenta $p_B^2 = M_B^2$, where possible contributions that are exponentially damped in the Euclidean region could become oscillatory. The validity of the OPE for inclusive decays is equivalent to the assumption of parton-hadron duality, and any violation of this assumption would imply the presence of terms which do not appear in the $1/m_b$ expansion [37]. However, fits of the HQE predictions to the data show no evidence for such terms and hence for duality violations. Thus duality or, equivalently, the validity of the OPE, is assumed in the analysis.

The OPE result for the total rate can be written schematically (the details of the expression can be found, *e.g.*, in Ref. 38) as

$$\begin{aligned} \Gamma = & |V_{cb}|^2 \hat{\Gamma}_0 m_b^5(\mu) (1 + A_{\text{ew}}) \times \\ & \left[z_0^{(0)}(r) + \frac{\alpha_s(\mu)}{\pi} z_0^{(1)}(r) + \left(\frac{\alpha_s(\mu)}{\pi} \right)^2 z_0^{(2)}(r) + \dots \right. \\ & + \frac{\mu_\pi^2}{m_b^2} \left(z_2^{(0)}(r) + \frac{\alpha_s(\mu)}{\pi} z_2^{(1)}(r) + \dots \right) \\ & \left. + \frac{\mu_G^2}{m_b^2} \left(y_2^{(0)}(r) + \frac{\alpha_s(\mu)}{\pi} y_2^{(1)}(r) + \dots \right) \right] \end{aligned}$$

$$\begin{aligned}
 & + \frac{\rho_D^3}{m_b^3} \left(z_3^{(0)}(r) + \frac{\alpha_s(\mu)}{\pi} z_3^{(1)}(r) + \dots \right) \\
 & + \frac{\rho_{LS}^3}{m_b^3} \left(y_3^{(0)}(r) + \frac{\alpha_s(\mu)}{\pi} y_3^{(1)}(r) + \dots \right) + \dots \Big] \quad (18)
 \end{aligned}$$

where $\eta_{\text{ew}} = 1 + A_{\text{ew}}$ denotes the electroweak corrections, r is the ratio m_c/m_b and the y_i and z_i are functions which appear in the perturbative expansion of the different orders of the heavy mass expansion. A similar expansion can be set up for moments of the distributions of charged-lepton energy, hadronic invariant mass and hadronic energy.

This expression is known up to order $1/m_b^5$, where the terms of order $1/m_b^n$ with $n > 2$ have been computed only at tree level [39–42]. The leading term is the parton model, which is known completely to order α_s and α_s^2 [43–45], and the terms of order $\alpha_s^{n+1}\beta_0^n$ (where β_0 is the first coefficient of the QCD β function, $\beta_0 = (33 - 2n_f)/3$) have been included by the usual BLM procedure [38,46,47]. Furthermore, the corrections of order $\alpha_s\mu_\pi^2/m_b^2$ have been computed [48,49].

Starting at order $1/m_b^3$ contributions with an infrared sensitivity to the charm mass m_c appear [41,50,51]. At order $1/m_b^3$ this “intrinsic charm” contribution is a $\log(m_c)$ in the coefficient of the Darwin term ρ_D^3 . At higher orders, terms such as $1/m_b^3 \times 1/m_c^2$ and $\alpha_s(m_c)1/m_b^3 \times 1/m_c$ appear, which are comparable in size to the contributions of order $1/m_b^4$.

The HQE parameters are given in terms of forward matrix elements; the parameters entering the expansion for orders up to $1/m_b^3$ are

$$\begin{aligned}
 \bar{\Lambda} &= M_B - m_b, \\
 \mu_\pi^2 &= -\langle B | \bar{b}(iD_\perp)^2 b | B \rangle, \\
 \mu_G^2 &= \langle B | \bar{b}(iD_\perp^\mu)(iD_\perp^\nu)\sigma_{\mu\nu} b | B \rangle, \\
 \rho_D^3 &= \langle B | \bar{b}(iD_{\perp\mu})(ivD)(iD_\perp^\nu) b | B \rangle, \\
 \rho_{LS}^3 &= \langle B | \bar{b}(iD_\perp^\mu)(ivD)(iD_\perp^\nu)\sigma_{\mu\nu} b | B \rangle. \quad (19)
 \end{aligned}$$

These parameters still depend on the heavy quark mass. Sometimes the infinite mass limits of these parameters $\bar{\Lambda} \rightarrow \bar{\Lambda}_{\text{HQET}}$, $\mu_\pi^2 \rightarrow -\lambda_1$, $\mu_G^2 \rightarrow 3\lambda_2$, $\rho_D^3 \rightarrow \rho_1$ and $\rho_{LS}^3 \rightarrow 3\rho_2$, are used instead. The hadronic parameters of the orders $1/m_b^4$ and $1/m_b^5$

have been defined and estimated in Ref. 42 while the five hadronic parameters s_i of the order $1/m_b^4$ can be found in Ref. 40; these have not yet been included in the fits.

The rates and the spectra depend strongly on m_b (or equivalently on $\overline{\Lambda}$), This makes the discussion of renormalization issues mandatory, since the size of the QCD corrections is strongly correlated with the definitions used for the quark masses. Using the pole mass definition for the heavy quark masses, it is well known that the corresponding perturbative series of decay rates does not converge very well, making a precision determination of $|V_{cb}|$ in such a scheme impossible.

The solution to this problem is to choose an appropriate “short-distance” mass definition. Frequently used mass definitions are the kinetic scheme [15], or the 1S scheme [52]. Both of these schemes have been applied to semileptonic $b \rightarrow c$ transitions, yielding comparable results and uncertainties.

The 1S scheme eliminates the b quark pole mass by relating it to the perturbative expression for the mass of the 1S state of the Υ system. The physical mass of the $\Upsilon(1S)$ contains non-perturbative contributions, which have been estimated in Ref. 53. These non-perturbative contributions are small; nevertheless, the best determination of the b quark mass in the 1S scheme is obtained from sum rules for $e^+e^- \rightarrow b\bar{b}$ [54].

Alternatively one may use a short-distance mass definition such as the $\overline{\text{MS}}$ mass $m_b^{\overline{\text{MS}}}(m_b)$. However, it has been argued that the scale m_b is unnaturally high for B decays, while for smaller scales $\mu \sim 1 \text{ GeV}$ $m_b^{\overline{\text{MS}}}(\mu)$ is under poor control. For this reason the so-called “kinetic mass” $m_b^{\text{kin}}(\mu)$, has been proposed. It is the mass entering the non-relativistic expression for the kinetic energy of a heavy quark, and is defined using heavy-quark sum rules [15].

Determination of HQE Parameters and $|V_{cb}|$

Several experiments have measured moments in $\overline{B} \rightarrow X_c \ell \overline{\nu}_\ell$ decays [55–63] as a function of the minimum lepton momentum. The measurements of the moments of the electron energy spectrum (0^{th} - 3^{rd}) and of the squared hadronic mass spectrum (0^{th} - 2^{nd}) have statistical uncertainties that are roughly equal to their systematic uncertainties. The sets of moments measured

by each experiment have strong correlations; the full statistical and systematic correlation matrices are required to allow these to be used in a global fit. Measurements of photon energy moments (0th-2nd) in $B \rightarrow X_s \gamma$ decays [64–68] as a function of the minimum accepted photon energy are still primarily statistics limited.

Global fits to the full set of moments [63,65,69–72] have been performed in the 1S and kinetic schemes. The semileptonic moments alone determine a linear combination of m_b and m_c very accurately but leave the orthogonal combination poorly determined [73]; additional input is required to allow a precise determination of m_b . This additional information can come from the radiative $B \rightarrow X_s \gamma$ moments, which provide complementary information on m_b and μ_π^2 , or from precise determinations of the charm quark mass [74,75]. The values obtained in the kinetic scheme fits [71] with these two constraints are consistent. Based on the charm quark mass constraint [76], $m_c^{\overline{\text{MS}}}(3 \text{ GeV}) = 0.986 \pm 0.013 \text{ GeV}$, a recent analysis [77] obtains

$$|V_{cb}| = (42.42 \pm 0.86) \times 10^{-3} \quad (20)$$

$$m_b^{\text{kin}} = 4.541 \pm 0.023 \text{ GeV} \quad (21)$$

$$\mu_\pi^2(\text{kin}) = 0.414 \pm 0.078 \text{ GeV}^2, \quad (22)$$

where the error on $|V_{cb}|$ includes experimental and theoretical uncertainties.

Theoretical uncertainties are estimated and included in performing the fits. Similar values for the parameters are obtained with a variety of assumptions about the theoretical uncertainties and their correlations. The χ^2/dof is substantially below unity in all fits, suggesting that the theoretical uncertainties may be overestimated. While one could obtain a satisfactory fit with smaller uncertainties, this would make the use of the extracted values for the HQE parameters in other processes unsafe. In any case, the low χ^2 shows no evidence for duality violations at a significant level. The mass in the $\overline{\text{MS}}$ scheme corresponding to Eq. (21) is $m_b^{\overline{\text{MS}}} = 4.17 \pm 0.04 \text{ GeV}$, which can be compared with a recent value obtained using relativistic sum

rules [76], $m_b^{\overline{\text{MS}}} = 4.163 \pm 0.016 \text{ GeV}$, and provides a non-trivial cross-check.

A fit in the 1S scheme [72] to the measured moments gives

$$|V_{cb}| = (41.96 \pm 0.45 \pm 0.07) \times 10^{-3} \quad (23)$$

$$m_b^{1\text{S}} = 4.691 \pm 0.037 \text{ GeV} \quad (24)$$

$$\lambda_1(1\text{S}) = -0.362 \pm 0.067 \text{ GeV}^2, \quad (25)$$

where the last error on $|V_{cb}|$ is due to the uncertainties in the B meson lifetimes. This fit uses semileptonic and radiative moments and constrains the chromomagnetic operator using the mass difference between the pseudoscalar and vector mesons (for both B and D); however, the fit does not include the constraint on m_c nor the full NNLO corrections.

The fits in the two renormalization schemes give consistent results for $|V_{cb}|$ and, after translation to a common renormalization scheme, for m_b and μ_π^2 . We take the arithmetic average of the $|V_{cb}|$ values and of the quoted uncertainties to find

$$|V_{cb}| = (42.2 \pm 0.7) \times 10^{-3} \text{ (inclusive)}. \quad (26)$$

The precision of the global fit results can be further improved by calculating higher order perturbative corrections to the coefficients of the HQE parameters, in particular the still missing $\alpha_s \mu_G^2$ corrections, which are presently only known for $B \rightarrow X_s \gamma$ [78]. The inclusion of still higher order moments may improve the sensitivity of the fits to higher order terms in the HQE.

Determination of $|V_{ub}|$

Summary: The determination of $|V_{ub}|$ is the focus of significant experimental and theoretical work. The determinations based on inclusive semileptonic decays using different calculational ansätze are consistent. The largest parametric uncertainty comes from the error on m_b . The best determinations of $|V_{ub}|$ from $\overline{B} \rightarrow \pi \ell \bar{\nu}_\ell$ decays come from combined fits to theory and experimental data as a function of q^2 ; the precision is limited by the form factor normalization.

The values obtained from inclusive and exclusive determinations are

$$|V_{ub}| = (4.41 \pm 0.15 \pm_{-0.17}^{+0.15}) \times 10^{-3} \quad (\text{inclusive}), \quad (27)$$

$$|V_{ub}| = (3.28 \pm 0.29) \times 10^{-3} \quad (\text{exclusive}). \quad (28)$$

The two determinations are independent, and the dominant uncertainties are on multiplicative factors. Given the marginal agreement between the inclusive and exclusive values their combination should be treated with caution. To combine these values, the inclusive and exclusive values are weighted by their relative errors and the uncertainties are treated as normally distributed. The resulting average has $p(\chi^2) = 0.01$, so we scale the error by $\sqrt{\chi^2/1} = 2.7$ to find

$$|V_{ub}| = (4.13 \pm 0.49) \times 10^{-3}. \quad (29)$$

Given the poor consistency between the two determinations, this average should be treated with caution.

$|V_{ub}|$ from inclusive decays

The theoretical description of inclusive $\overline{B} \rightarrow X_u \ell \overline{\nu}_\ell$ decays is based on the Heavy Quark Expansion, as for $\overline{B} \rightarrow X_c \ell \overline{\nu}_\ell$ decays, and leads to a predicted total decay rate with uncertainties below 5% [79,80]. Unfortunately, the total decay rate is hard to measure due to the large background from CKM-favored $\overline{B} \rightarrow X_c \ell \overline{\nu}_\ell$ transitions. Technically, the calculation of the partial decay rate in regions of phase space where $\overline{B} \rightarrow X_c \ell \overline{\nu}_\ell$ decays are suppressed requires the introduction of a non-perturbative distribution function, the “shape function” (SF) [81,82], whose form is unknown. The shape function becomes important when the light-cone momentum component $P_+ \equiv E_X - |P_X|$ is not large compared to Λ_{QCD} . This additional difficulty can be addressed in two complementary ways. The leading shape function can either be measured in the radiative decay $\overline{B} \rightarrow X_s \gamma$, or be modeled with constraints on the 0th-2nd moments, and the results applied to the calculation of the $\overline{B} \rightarrow X_u \ell \overline{\nu}_\ell$ partial decay rate [83–85]; in such an approach the largest challenges are for the theory. Alternatively, measurements of $\overline{B} \rightarrow X_u \ell \overline{\nu}_\ell$ partial decay rates can be extended

further into the $\overline{B} \rightarrow X_c \ell \overline{\nu}_\ell$ -allowed region, enabling a simplified theoretical (pure HQE) treatment [86] but requiring precise experimental knowledge of the $\overline{B} \rightarrow X_c \ell \overline{\nu}_\ell$ background.

At leading order a single shape function appears, which is universal for all heavy-to-light transitions [81,82], and thus it can be measured in $\overline{B} \rightarrow X_s \gamma$ decays. However, at sub-leading order in $1/m_b$ several shape functions appear [87] rendering a simple comparison of semileptonic and radiative B decays impossible.

The form of the SFs cannot be calculated from first principles. Prescriptions that relate directly the partial rates for $\overline{B} \rightarrow X_s \gamma$ and $\overline{B} \rightarrow X_u \ell \overline{\nu}_\ell$ decays are available [88–91]; however, this approach is limited to the leading order in $1/m_b$.

Existing approaches have tended to use parameterizations of the leading SF that respect constraints on the zeroth, first and second moments, which are given in terms of the HQE parameters $\overline{\Lambda} = M_B - m_b$ and μ_π^2 , respectively. The relations between SF moments and the HQE parameters are known to second order in α_s [92]. As a result, measurements of HQE parameters from global fits to $\overline{B} \rightarrow X_c \ell \overline{\nu}_\ell$ and $\overline{B} \rightarrow X_s \gamma$ moments can be used to constrain the SF moments, as well as provide accurate values of m_b and other parameters for use in determining $|V_{ub}|$.

A recent development is to use appropriate basis functions to approximate the shape function, thereby also including the known short-distance contributions as well as the renormalization properties of the SF [93], in order to allow a global fit of all inclusive B meson decay data.

The calculations that are used for the fits performed by HFAG are documented in Refs. [83] (BLNP), [94] (GGOU), [95] (DGE) and [86] (BLL).

The triple differential rate in the variables

$$P_l = M_B - 2E_l, \quad P_- = E_X + |\vec{P}_X|, \quad P_+ = E_X - |\vec{P}_X| \quad (30)$$

is

$$\frac{d^3\Gamma}{dP_+ dP_- dP_l} = \frac{G_F^2 |V_{ub}|^2}{16\pi^2} (M_B - P_+) \quad (31)$$

$$\left\{ (P_- - P_l)(M_B - P_- + P_l - P_+) \mathcal{F}_1 \right. \\ \left. + (M_B - P_-)(P_- - P_+) \mathcal{F}_2 + (P_- - P_l)(P_l - P_+) \mathcal{F}_3 \right\}.$$

The “structure functions” \mathcal{F}_i can be calculated using factorization theorems that have been proven to subleading order in the $1/m_b$ expansion.

The BLNP [83] calculation uses these factorization theorems to write the \mathcal{F}_i in terms of perturbatively calculable hard coefficients H and jet functions J , which are convolved with the (soft) light-cone distribution functions S , the shape functions of the B meson. The partial calculation of the $\mathcal{O}(\alpha_s^2)$ contributions in Ref. 96 has recently been completed [97]. However, the full calculation is not yet included in the fit.

The leading order term in the $1/m_b$ expansion of the \mathcal{F}_i contains a single non-perturbative function and is calculated to subleading order in α_s , while at subleading order in the $1/m_b$ expansion there are several independent non-perturbative functions which have been calculated only at tree level in the α_s expansion.

To extract the non-perturbative input one can study the photon energy spectrum in $B \rightarrow X_s \gamma$ [85]. This spectrum is known to a similar accuracy as the P_+ spectrum in $B \rightarrow X_u \ell \bar{\nu}_\ell$. Going to subleading order in the $1/m_b$ expansion requires the modeling of subleading SFs, a large variety of which were studied in Ref. 83.

A distinct approach (GGOU) [94] uses a hard, Wilsonian cut-off that matches the definition of the kinetic mass. The non-perturbative input is similar to what is used in BLNP, but the shape functions are defined differently. In particular, they are defined at finite m_b and depend on the light-cone component k_+ of the b quark momentum and on the momentum transfer q^2 to the leptons. These functions include sub-leading effects to all orders; as a result they are non-universal, with one shape function corresponding to each structure function in Eq. (31). Their k_+ moments can be computed in the OPE and related to observables and to the shape functions defined in Ref. 83.

Going to subleading order in α_s requires the definition of a renormalization scheme for the HQE parameters and for the

SF. It has been noted that the relation between the moments of the SF and the forward matrix elements of local operators is plagued by ultraviolet problems which require additional renormalization. A possible scheme for improving this behavior has been suggested in Refs. [83,85], which introduce a particular definition of the quark mass (the so-called shape function scheme) based on the first moment of the measured spectrum. Likewise, the HQE parameters can be defined from measured moments of spectra, corresponding to moments of the SF.

One can also attempt to calculate the SF by using additional assumptions. One possible approach (DGE) is the so-called “dressed gluon exponentiation” [95], where the perturbative result is continued into the infrared regime using the renormalon structure obtained in the large β_0 limit, where β_0 has been defined following Eq. (18).

While attempts to quantify the SF are important, the impact of uncertainties in the SF is significantly reduced in some recent measurements that cover a larger portion of the $\overline{B} \rightarrow X_u \ell \overline{\nu}_\ell$ phase space. Several measurements using a combination of cuts on the leptonic momentum transfer q^2 and the hadronic invariant mass m_X as suggested in Ref. 98 have been made. Measurements of the electron spectrum in $\overline{B} \rightarrow X_u \ell \overline{\nu}_\ell$ decays have been made down to momenta of 1.9 GeV, where SF uncertainties are not dominant; however, determining $\overline{B} \rightarrow X_u \ell \overline{\nu}_\ell$ partial rates in charm-dominated regions can bring in a strong dependence on the modeling of the $\overline{B} \rightarrow X_u \ell \overline{\nu}_\ell$ spectrum, which is problematic. The measurements quoted below have used a variety of functional forms to parameterize the leading SF; in no case does this lead to more than a 2% uncertainty on $|V_{ub}|$.

Weak Annihilation [99,100,94] (WA) can in principle contribute significantly in the high- q^2 region accepted by measurements of $\overline{B} \rightarrow X_u \ell \overline{\nu}_\ell$ decays. Estimates based on semileptonic D_s decays [100,51,86] lead to a $\sim 2\%$ uncertainty on the total $\overline{B} \rightarrow X_u \ell \overline{\nu}_\ell$ rate from the $\Upsilon(4S)$. The q^2 spectrum of the WA contribution is not well known, but from the OPE it is expected to contribute predominantly at high q^2 . More recent investigations [51,101,102] indicate that WA is a small effect, but may

become a significant source of uncertainty for $|V_{ub}|$ measurements that only accept a small fraction of the full $\overline{B} \rightarrow X_u \ell \overline{\nu}_\ell$ phase space. Model-dependent limits on WA were determined in Ref. 103, where the CLEO data were fitted to combinations of WA models and a spectator $\overline{B} \rightarrow X_u \ell \overline{\nu}_\ell$ component and background. More direct experimental constraints [104] on WA have been made by comparing the $\overline{B} \rightarrow X_u \ell \overline{\nu}_\ell$ decay rates of charged and neutral B mesons, although these constraints are not sensitive to the isoscalar contribution to WA.

Measurements

We summarize the measurements used in the determination of $|V_{ub}|$ below. Given the improved precision and more rigorous theoretical interpretation of the recent measurements, earlier determinations [105–108] will not be further considered in this review.

Inclusive electron momentum measurements [109–111] reconstruct a single charged electron to determine a partial decay rate for $\overline{B} \rightarrow X_u \ell \overline{\nu}_\ell$ near the kinematic endpoint. This results in a high $\mathcal{O}(50\%)$ selection efficiency and only modest sensitivity to the modeling of detector response. The decay rate can be cleanly extracted for $E_e > 2.3$ GeV, but this is deep in the SF region, where theoretical uncertainties are large. Measurements down to 2.0 or 1.9 GeV have a low ($< 1/10$) signal-to-background (S/B) ratio. The inclusive electron momentum spectrum from $B\overline{B}$ events, after subtraction of the $e^+e^- \rightarrow q\overline{q}$ continuum background, is fitted to a model $\overline{B} \rightarrow X_u \ell \overline{\nu}_\ell$ spectrum and several components ($D\ell\overline{\nu}_\ell$, $D^*\ell\overline{\nu}_\ell$, ...) of the $\overline{B} \rightarrow X_c \ell \overline{\nu}_\ell$ background; the dominant uncertainties are related to this subtraction and modelling. The resulting $|V_{ub}|$ values for various E_e cuts are given in Table 1.

An untagged “neutrino reconstruction” measurement [112] from BABAR uses a combination [113] of a high-energy electron with a measurement of the missing momentum vector. This allows a much higher $S/B \sim 0.7$ at the same E_e cut and a $\mathcal{O}(5\%)$ selection efficiency, but at the cost of a smaller accepted phase space for $\overline{B} \rightarrow X_u \ell \overline{\nu}_\ell$ decays and uncertainties

associated with the determination of the missing momentum. The corresponding values for $|V_{ub}|$ are given in Table 1.

The large samples accumulated at the B factories allow studies in which one B meson is fully reconstructed and the recoiling B decays semileptonically [114–118]. The experiments can fully reconstruct a “tag” B candidate in about 0.5% (0.3%) of B^+B^- ($B^0\bar{B}^0$) events. An electron or muon with center-of-mass momentum above 1.0 GeV is required amongst the charged tracks not assigned to the tag B and the remaining particles are assigned to the X_u system. The full set of kinematic properties (E_ℓ , m_X , q^2 , etc.) are available for studying the semileptonically decaying B , making possible selections that accept up to 90% of the full $\bar{B} \rightarrow X_u \ell \bar{\nu}_\ell$ rate. Despite requirements (e.g. on the square of the missing mass) aimed at rejecting events with additional missing particles, undetected or mis-measured particles from $\bar{B} \rightarrow X_c \ell \bar{\nu}_\ell$ decay (e.g., K_L^0 and additional neutrinos) remain an important source of uncertainty. Measurements with the largest kinematic acceptance (i.e. $E_\ell > 1$ GeV) lead to the smallest theoretical and overall uncertainties on $|V_{ub}|$.

BABAR [114] and BELLE [115,116] have measured partial rates with cuts on m_X , m_X and q^2 , P_+ and E_ℓ based on large samples of $B\bar{B}$ events; the corresponding $|V_{ub}|$ values are given in Table 1. In each case the experimental systematics have significant contributions from the modeling of $\bar{B} \rightarrow X_u \ell \bar{\nu}_\ell$ and $\bar{B} \rightarrow X_c \ell \bar{\nu}_\ell$ decays and from the detector response to charged particles, photons and neutral hadrons.

Determination of $|V_{ub}|$

The determination of $|V_{ub}|$ from the measured partial rates requires input from theory. The BLNP, GGOU and DGE calculations described previously are used to determine $|V_{ub}|$ from all measured partial $\bar{B} \rightarrow X_u \ell \bar{\nu}_\ell$ rates; the values [28] are given in Table 1. The HFAG averages quoted here are based on the following m_b values: $m_b^{SF} = 4.588 \pm 0.025$ GeV for BLNP, $m_b^{\text{kin}} = 4.560 \pm 0.023$ GeV for GGOU, and $m_b^{\overline{MS}} = 4.194 \pm 0.043$ GeV for DGE. The m_b^{kin} value is determined in a global fit to moments in the kinetic scheme; this value is translated into m_b^{SF} and $m_b^{\overline{MS}}$ at fixed order in α_s . These input values are based on an earlier determination of m_b^{kin} than is quoted in

equation Eq. (21); using the latest value would increase the $|V_{ub}|$ averages by 1-2%.

As an illustration of the relative sizes of the uncertainties entering $|V_{ub}|$ we give the error breakdown for the GGOU average: statistical—2.0%; experimental—1.7%; $\overline{B} \rightarrow X_c \ell \overline{\nu}_\ell$ modeling—1.3%; $\overline{B} \rightarrow X_u \ell \overline{\nu}_\ell$ modeling—1.9%; HQE parameters —1.9%; higher-order corrections—1.4%; q^2 modeling—1.3%; Weak Annihilation— $^{+0}_{-1.9}$ %; SF form—0.2%. The uncertainty on m_b dominates the uncertainty on $|V_{ub}|$ from HQE parameters, but no longer dominates the overall uncertainty.

The correlations amongst the multiple BABAR recoil-based measurements [114] are fully accounted for in the average. The statistical correlations amongst the other measurements used in the average are tiny (due to small overlaps among signal events and large differences in S/B ratios) and have been ignored. Correlated systematic and theoretical errors are taken into account, both within an experiment and between experiments.

Table 1: $|V_{ub}|$ (in units of 10^{-5}) from inclusive $\overline{B} \rightarrow X_u \ell \overline{\nu}_\ell$ measurements. The first uncertainty on $|V_{ub}|$ is experimental, while the second includes both theoretical and HQE parameter uncertainties. The values are listed in order of increasing f_u (0.19 to 0.90); those below the horizontal bar are based on recoil methods.

Ref.	cut	BLNP	GGOU	DGE
[109]	$E_e > 2.1$	419 ± 49 $^{+26}_{-34}$	393 ± 46 $^{+22}_{-29}$	382 ± 45 $^{+23}_{-26}$
[112]	$E_e - q^2$	466 ± 31 $^{+31}_{-36}$	not available	432 ± 29 $^{+24}_{-29}$
[111]	$E_e > 2.0$	448 ± 25 $^{+27}_{-28}$	429 ± 24 $^{+18}_{-24}$	428 ± 24 $^{+22}_{-24}$
[110]	$E_e > 1.9$	488 ± 45 $^{+24}_{-27}$	475 ± 44 $^{+17}_{-22}$	479 ± 44 $^{+21}_{-24}$
[114]	$m_X - q^2$	425 ± 23 $^{+23}_{-25}$	417 ± 22 $^{+22}_{-25}$	419 ± 22 $^{+18}_{-19}$
[114]	P_+	402 ± 25 $^{+24}_{-23}$	375 ± 23 $^{+30}_{-32}$	410 ± 25 $^{+37}_{-28}$
[114]	m_X	397 ± 22 $^{+20}_{-20}$	394 ± 22 $^{+16}_{-17}$	416 ± 23 $^{+26}_{-22}$
[114]	$E_e > 1$	428 ± 24 $^{+18}_{-20}$	435 ± 24 $^{+09}_{-10}$	440 ± 24 $^{+12}_{-13}$
[116]	$E_e > 1$	447 ± 27 $^{+19}_{-21}$	454 ± 27 $^{+10}_{-11}$	460 ± 27 $^{+11}_{-13}$
		440 ± 15 $^{+19}_{-21}$	439 ± 15 $^{+12}_{-14}$	445 ± 15 $^{+15}_{-16}$

The theoretical calculations produce very similar results for $|V_{ub}|$; the standard deviation of the theory predictions for the endpoint rate is 4.6%, for the m_X - q^2 rate is 2.2%, and for the $E_e > 1$ GeV rate is 0.8%. The $|V_{ub}|$ values do not show a marked trend versus the kinematic acceptance, f_u , for $\overline{B} \rightarrow X_u \ell \overline{\nu}_\ell$ decays. The p -values of the averages are in the range 34-44%, indicating that the ratios of calculated partial widths in the different phase space regions are in good agreement with ratios of measured partial branching fractions.

All calculations yield compatible $|V_{ub}|$ values and similar error estimates. We take the arithmetic mean of the values and errors to find

$$|V_{ub}| = (4.41 \pm 0.15_{\text{exp}} \text{ }^{+0.15}_{-0.17}_{\text{theo}}) \times 10^{-3} \quad (\text{inclusive}). \quad (32)$$

Hadronization uncertainties also impact the $|V_{ub}|$ determination. The theoretical expressions are valid at the parton level and do not incorporate any resonant structure (*e.g.* $\overline{B} \rightarrow \pi \ell \overline{\nu}_\ell$); this must be added to the simulated $\overline{B} \rightarrow X_u \ell \overline{\nu}_\ell$ event samples, since the detailed final state multiplicity and structure impacts the estimates of experimental acceptance and efficiency. The experiments have adopted procedures to input resonant structure while preserving the appropriate behavior in the kinematic variables (q^2, E_ℓ, m_X) averaged over the sample, but these prescriptions are not unique. The resulting uncertainties have been estimated to be ~ 1 -2% on $|V_{ub}|$.

A separate class of analyses follows the strategy discussed in Refs. [88–91], where integrals of differential distributions in $\overline{B} \rightarrow X_u \ell \overline{\nu}_\ell$ decays are compared with corresponding integrals in $\overline{B} \rightarrow X_s \gamma$ decays to extract $|V_{ub}|$, thereby eliminating the need to model the leading shape function. A study [117] using the measured BABAR electron spectrum in $\overline{B} \rightarrow X_u \ell \overline{\nu}_\ell$ decays provides $|V_{ub}|$ determinations using all available “SF-free” calculations; the resulting $|V_{ub}|$ values have total uncertainties of $\sim 12\%$ and are compatible with the average quoted above.

The BLL [98] calculation can be used for measurements [115,118,119] with cuts on m_X and q^2 . Using the same HQE parameter input as above yields a $|V_{ub}|$ value of $(4.62 \pm 0.20 \pm$

$0.29) \times 10^{-3}$, which is about 7% higher than the values obtained from the calculations used in Table 1 for these same measurements.

Status and outlook

At present, as indicated by the average given above, the uncertainty on $|V_{ub}|$ from inclusive decays is at the 5% level. The uncertainty on m_b was discussed in detail above. The uncertainties quoted in the calculations due to matching scales, higher order corrections, etc., are at the few percent level on $|V_{ub}|$. While these uncertainties are inherently difficult to quantify, the calculations take different approaches and yet yield similar estimates. The recent calculation of the full NNLO contributions in Ref. 97 indicates, that the NNLO terms are indeed dominated by the contributions of the order $\alpha_s^2\beta_0$, which are included in both the GGOU and DGE fits. To this end, the sizeable shift of V_{ub} in the BLNP approach induced by including the partial $\mathcal{O}(\alpha_s^2)$ corrections computed in [96] seems to be an artifact.

Experimental uncertainties have been assessed independently by BaBar and Belle. An important common source of uncertainty comes from the modelling of hadronization in inclusive $\overline{B} \rightarrow X_u \ell \overline{\nu}_\ell$ decays. Better measurements of these exclusive decays, as in Ref. 120, are helpful in this regard, as would improved knowledge of the main $\overline{B} \rightarrow X_c \ell \overline{\nu}_\ell$ decays.

$|V_{ub}|$ from exclusive decays

Exclusive charmless semileptonic decays offer a complementary means of determining $|V_{ub}|$. For the experiments, the specification of the final state provides better background rejection, but the lower branching fraction reflects itself in lower yields compared with inclusive decays. For theory, the calculation of the form factors for $\overline{B} \rightarrow X_u \ell \overline{\nu}_\ell$ decays is challenging, but brings in a different set of uncertainties from those encountered in inclusive decays. In this review we focus on $\overline{B} \rightarrow \pi \ell \overline{\nu}_\ell$, as it is the most promising mode for both experiment and theory, and recent improvements have been made in both areas. Measurements of other exclusive states can be found in Refs. [121–127].

$\overline{B} \rightarrow \pi \ell \overline{\nu}_\ell$ form factor calculations

The relevant form factors for the decay $\overline{B} \rightarrow \pi \ell \overline{\nu}_\ell$ are usually defined as

$$\langle \pi(p_\pi) | V^\mu | B(p_B) \rangle = \tag{33}$$

$$f_+(q^2) \left[p_B^\mu + p_\pi^\mu - \frac{m_B^2 - m_\pi^2}{q^2} q^\mu \right] + f_0(q^2) \frac{m_B^2 - m_\pi^2}{q^2} q^\mu$$

in terms of which the rate becomes (in the limit $m_\ell \rightarrow 0$)

$$\frac{d\Gamma}{dq^2} = \frac{G_F^2 |V_{ub}|^2}{24\pi^3} |p_\pi|^3 |f_+(q^2)|^2, \tag{34}$$

where p_π is the pion momentum in the B meson rest frame.

Currently available non-perturbative methods for the calculation of the form factors include lattice QCD (LQCD) and light-cone sum rules (LCSR). The two methods are complementary in phase space, since the lattice calculation is restricted to the kinematical range of high momentum transfer q^2 to the leptons, while light-cone sum rules provide information near $q^2 = 0$. Interpolations between these two regions can be constrained by unitarity and analyticity.

Unquenched simulations, i.e. where quark loop effects are fully incorporated, have become quite common, and the commonly used results based on these simulations for the $\overline{B} \rightarrow \pi \ell \overline{\nu}_\ell$ form factors have been obtained by the Fermilab/MILC collaboration [128] and the HPQCD collaboration [129]. The two calculations differ in the way the b quark is simulated, with HPQCD using nonrelativistic QCD and Fermilab/MILC the so-called Fermilab heavy-quark method; they agree within the quoted errors.

The extrapolation to small values of q^2 can be performed by using analyticity and unitarity bounds. Making use of the heavy-quark limit, stringent constraints on the shape of the form factor can be derived [130], and the conformal mapping of the kinematical variables onto the complex unit disc yields a rapidly converging series in the variable

$$z = \frac{\sqrt{t_+ - t_-} - \sqrt{t_+ - q^2}}{\sqrt{t_+ - t_-} + \sqrt{t_+ - q^2}}$$

where $t_{\pm} = (M_B \pm m_{\pi})^2$. The use of lattice data in combination with a data point at small q^2 from SCET or sum rules provides a stringent constraint on the shape of the form factor [131]. The form factor parametrization given in Ref. 131 has been applied to the extraction of $|V_{ub}|$ from $B \rightarrow \pi \ell \bar{\nu}_{\ell}$ using lattice data in Ref. 128.

Much work remains to be done, since the current combined statistical plus systematic errors in the lattice results are still at the $\sim 10\%$ level on $|V_{ub}|$ and need to be reduced. Reduction of errors to the $\sim 5\text{-}6\%$ level for $|V_{ub}|$ will be feasible within the next few years, with the inclusion of numerical data at lighter pion masses and finer lattice spacings, as well as possibly two-loop or nonperturbative matching between lattice and continuum heavy-to-light current operators.

Another established non-perturbative approach to obtain the form factors is through Light-Cone QCD Sum Rules (LCSR), where the heavy mass limit has been discussed from the point of view of SCET in Ref. 132. The sum-rule approach provides an approximation for the product $f_B f_+(q^2)$, valid in the region $0 < q^2 < \sim 12 \text{ GeV}^2$. The determination of $f_+(q^2)$ itself requires knowledge of the decay constant f_B , which usually is obtained by replacing f_B by its two-point QCD (SVZ) sum rule [133] in terms of perturbative and condensate contributions. The advantage of this procedure is the approximate cancellation of various theoretical uncertainties in the ratio $(f_B f_+)/f_B$. The LCSR for $f_B f_+$ is based on the light-cone OPE of the relevant vacuum-to-pion correlation function, calculated in full QCD at finite b -quark mass. The resulting expressions actually comprise a triple expansion: in the twist t of the operators near the light-cone, in α_s , and in the deviation of the pion distribution amplitudes from their asymptotic form, which is fixed from conformal symmetry.

There are multiple sources of uncertainties in the LCSR calculation, which are discussed in Refs. [134,135]. Currently, a total uncertainty slightly larger than 10% on $|V_{ub}|$ is extracted

from a LCSR calculation of

$$\begin{aligned} \Delta\zeta(0, q_{max}^2) &= \frac{G_F^2}{24\pi^3} \int_0^{q_{max}^2} dq^2 p_\pi^3 |f_+(q^2)|^2 \\ &= \frac{1}{|V_{ub}|^2 \tau_{B_0}} \int_0^{q_{max}^2} dq^2 \frac{d\mathcal{B}(B \rightarrow \pi \ell \nu)}{dq^2} \end{aligned} \quad (35)$$

which gives [136]

$$\Delta\zeta(0, 12 \text{ GeV}^2) = 4.59_{-0.85}^{+1.00} \text{ ps}^{-1}. \quad (36)$$

The recent calculation of two loop contributions to the LCQCD sum rules [137] only yields a small effect.

It is interesting to note that the results from LQCD extrapolate smoothly onto the LCSR results when employing the parametrizations based on conformal mappings [131,138]. This increases confidence in the theoretical predictions for the rate of $\bar{B} \rightarrow \pi \ell \bar{\nu}_\ell$.

$\bar{B} \rightarrow \pi \ell \bar{\nu}_\ell$ measurements

The $\bar{B} \rightarrow \pi \ell \bar{\nu}_\ell$ measurements fall into two broad classes: untagged, in which case the reconstruction of the missing momentum of the event serves as an estimator for the unseen neutrino, and tagged, in which the second B meson in the event is fully reconstructed in either a hadronic or semileptonic decay mode. The tagged measurements have high and uniform acceptance, S/B as high as 10, but low statistics. The untagged measurements have somewhat higher background levels (S/B < 1) and make slightly more restrictive kinematic cuts, but have adequate statistics to measure the q^2 dependence of the form factor.

Table 2: Total and partial branching fractions for $\bar{B}^0 \rightarrow \pi^+ \ell^- \bar{\nu}_\ell$. B-tagged analyses are indicated (SL for *semileptonic*, had for *hadronic*). The uncertainties are from statistics and systematics. Measurements of $\mathcal{B}(B^- \rightarrow \pi^0 \ell^- \bar{\nu}_\ell)$ have been multiplied by a factor $2\tau_{B^0}/\tau_{B^+}$ to obtain the values below.

	$\mathcal{B} \times 10^4$	$\mathcal{B}(q^2 > 16) \times 10^4$
CLEO π^+, π^0 [125]	$1.38 \pm 0.15 \pm 0.11$	$0.41 \pm 0.08 \pm 0.04$
BABAR π^+, π^0 [126]	$1.41 \pm 0.05 \pm 0.08$	$0.32 \pm 0.02 \pm 0.03$
BABAR π^+ [127]	$1.44 \pm 0.04 \pm 0.06$	$0.37 \pm 0.02 \pm 0.02$
BELLE π^+, π^0 [139]	$1.48 \pm 0.04 \pm 0.07$	$0.40 \pm 0.02 \pm 0.02$
BELLE SL π^+ [140]	$1.41 \pm 0.19 \pm 0.15$	$0.37 \pm 0.10 \pm 0.04$
BELLE SL π^0 [140]	$1.41 \pm 0.26 \pm 0.15$	$0.37 \pm 0.15 \pm 0.04$
BELLE had π^+ [120]	$1.49 \pm 0.09 \pm 0.07$	$0.45 \pm 0.05 \pm 0.02$
BELLE had π^0 [120]	$1.48 \pm 0.15 \pm 0.08$	$0.36 \pm 0.07 \pm 0.02$
BABAR SL π^+ [141]	$1.39 \pm 0.21 \pm 0.08$	$0.46 \pm 0.13 \pm 0.03$
BABAR SL π^0 [141]	$1.78 \pm 0.28 \pm 0.15$	$0.44 \pm 0.17 \pm 0.06$
BABAR had π^+ [142]	$1.07 \pm 0.27 \pm 0.19$	$0.65 \pm 0.20 \pm 0.13$
BABAR had π^0 [142]	$1.52 \pm 0.41 \pm 0.30$	$0.48 \pm 0.22 \pm 0.12$
Average	$1.45 \pm 0.02 \pm 0.04$	$0.38 \pm 0.01 \pm 0.01$

CLEO has analyzed $\bar{B} \rightarrow \pi \ell \bar{\nu}_\ell$ and $\bar{B} \rightarrow \rho \ell \bar{\nu}_\ell$ using an untagged analysis [125]. Similar analyses have been done at BABAR [126,127] and BELLE [139]. The leading systematic uncertainties in the untagged $\bar{B} \rightarrow \pi \ell \bar{\nu}_\ell$ analyses are associated with modeling the missing momentum reconstruction, with backgrounds from $\bar{B} \rightarrow X_u \ell \bar{\nu}_\ell$ decays and $e^+e^- \rightarrow q\bar{q}$ continuum events, and with varying the form factor for the $\bar{B} \rightarrow \rho \ell \bar{\nu}_\ell$ decay. The values obtained for the full and partial branching fractions [28] are listed in Table 2 above the horizontal line. These BABAR and BELLE measurements provide the differential $\bar{B} \rightarrow \pi \ell \bar{\nu}_\ell$ rate versus q^2 , shown in Fig. 1, which is used in the determination of $|V_{ub}|$ discussed below.

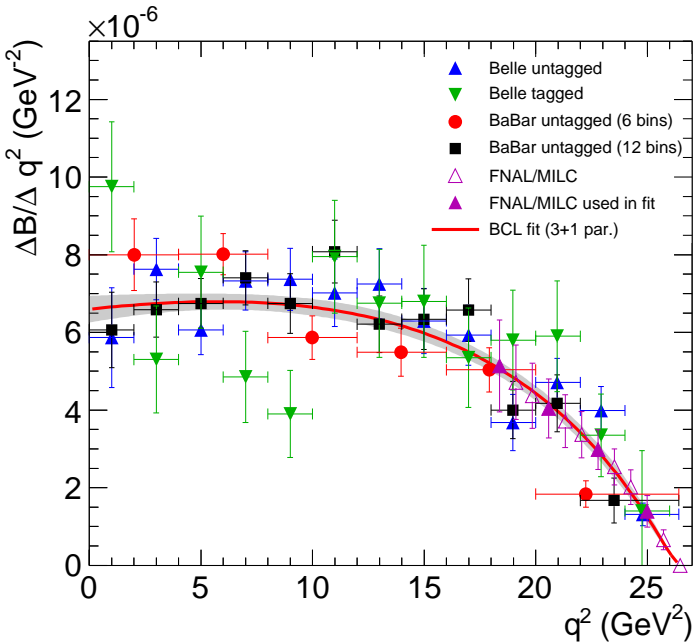


Figure 1: The untagged measurements of the differential $\overline{B} \rightarrow \pi \ell \bar{\nu}_\ell$ branching fraction versus q^2 that are used together with lattice calculations in the determination of $|V_{ub}|$.

Analyses [140,141] based on reconstructing a B in the $\overline{D}^{(*)} \ell^+ \nu_\ell$ decay mode and looking for a $\overline{B} \rightarrow \pi \ell \bar{\nu}_\ell$ or $\overline{B} \rightarrow \rho \ell \bar{\nu}_\ell$ decay amongst the remaining particles in the event make use of the fact that the B and \overline{B} are back-to-back in the $\Upsilon(4S)$ frame to construct a discriminant variable that provides a signal-to-noise ratio above unity for all q^2 bins. A related technique was discussed in Ref. 143. BABAR [141] and [120] have also used their samples of B mesons reconstructed in hadronic decay modes to measure exclusive charmless semileptonic decays giving very clean but low-yield samples. The resulting full and partial branching fractions are given in Table 2. The averages take account of correlations and common systematic uncertainties, and have $p(\chi^2) > 0.5$ in each case.

$|V_{ub}|$ can be obtained from the average $\overline{B} \rightarrow \pi \ell \bar{\nu}_\ell$ branching fraction and the measured q^2 spectrum. Using the average [28] of partial branching fractions in the $q^2 < 12 \text{ GeV}^2$ region,

$(0.81 \pm 0.02 \pm 0.02) \times 10^{-4}$, along with an LCSR calculation of the theoretical rate [136] gives

$$|V_{ub}| = (3.41 \pm 0.06_{\text{exp}}^{+0.37}_{-0.32} \text{theo}) \times 10^{-3} \quad (\text{LCSR}, q^2 < 12 \text{ GeV}^2). \quad (37)$$

Fits to the measured q^2 spectrum using a theoretically motivated parameterization (e.g. "BCL" from Ref. 138) remove most of the model dependence from theoretical uncertainties in the shape of the spectrum. Recent determinations [28,128] of $|V_{ub}|$ from $\overline{B} \rightarrow \pi \ell \bar{\nu}_\ell$ decays have used simultaneous fits (see also Ref. 144) to the experimental partial rate and lattice points versus q^2 . A fit [28] to the untagged measurements incorporates the full statistical and systematic uncertainties in the measured spectrum and uses four lattice points in the region $q^2 > 16 \text{ GeV}^2$, taking into account their correlations. The fit, shown in Fig. 1, has $p(\chi^2) = 2.2\%$. If the tagged measurements, which are less consistent in the $q^2 < 8 \text{ GeV}^2$ region, are included, the fit gives $p(\chi^2) < 0.01\%$. We quote the result from the untagged measurements and add the difference (0.09×10^{-3}) between the $|V_{ub}|$ values from the two fits as an additional uncertainty to find

$$|V_{ub}| = (3.28 \pm 0.29) \times 10^{-3} \quad (\text{exclusive}). \quad (38)$$

The largest contributions to the uncertainty come from lattice systematic and statistical errors, which will be further improved in the future.

$\overline{B} \rightarrow D^{(*)} \tau \bar{\nu}_\ell$

Summary: Semileptonic decays to third-generation leptons provide sensitivity to non-standard model amplitudes, such as from a charged Higgs boson [145]. The ratios of branching fractions of semileptonic decays involving tau leptons to those involving e/μ , $\mathcal{R}_{D^{(*)}} \equiv \mathcal{B}(\overline{B} \rightarrow D^{(*)} \tau \bar{\nu}_\ell) / \mathcal{B}(\overline{B} \rightarrow D^{(*)} \ell \bar{\nu}_\ell)$, are predicted with good precision in the standard model: [146]

$$\begin{aligned} \mathcal{R}_D^{\text{SM}} &= 0.297 \pm 0.017 \\ \mathcal{R}_{D^*}^{\text{SM}} &= 0.252 \pm 0.003. \end{aligned} \quad (39)$$

Measurements [146–150] of these ratios yield higher values; using B-tagged measurements only we find

$$\begin{aligned}\mathcal{R}_D^{\text{meas}} &= 0.462 \pm 0.067 \\ \mathcal{R}_{D^*}^{\text{meas}} &= 0.341 \pm 0.029\end{aligned}\quad (40)$$

These values exceed standard model predictions by 2.4σ and 3.0σ , respectively. A variety of new physics models have been proposed [145,151–154] to explain this excess. The potential impact of any new physics in this decay mode on the $|V_{ub}|$ and $|V_{cb}|$ results given above is expected to be negligible.

Sensitivity of $\bar{B} \rightarrow D^{(*)}\tau\bar{\nu}_\ell$ to additional amplitudes

In addition to the helicity amplitudes present for decays to $e\bar{\nu}_e$ and $\mu\bar{\nu}_\mu$, decays proceeding through $\tau\bar{\nu}_\tau$ include a scalar amplitude H_s . The differential decay rate is given by [155]

$$\begin{aligned}\frac{d\Gamma}{dq^2} &= \frac{G_F^2 |V_{cb}|^2 |\mathbf{p}_{D^{(*)}}^*|^2}{96\pi^3 m_B^2} \left(1 - \frac{m_\tau^2}{q^2}\right)^2 \\ &\left[(|H_+|^2 + |H_-|^2 + |H_0|^2) \left(1 + \frac{m_\tau^2}{2q^2}\right) + \frac{3m_\tau^2}{2q^2} |H_s|^2 \right],\end{aligned}\quad (41)$$

where $|\mathbf{p}_{D^{(*)}}^*|$ is the 3-momentum of the $D^{(*)}$ in the \bar{B} rest frame and the helicity amplitudes depend on q^2 . All four helicity amplitudes contribute to $\bar{B} \rightarrow D^* \tau \bar{\nu}_\ell$, while only H_0 and H_s contribute to $\bar{B} \rightarrow D \tau \bar{\nu}_\ell$; as a result, new physics contributions tend to produce larger effects in the latter mode. The use of the ratios of decay rates, $\mathcal{R}_{D^{(*)}}$, allows a partial cancellation of uncertainties in standard model form factors, and reduces the impact of many experimental uncertainties.

The (semi)-leptonic B decays into a τ lepton provide a stringent test of the two-Higgs doublet model of type II (2HDMII), i.e. where the two Higgs doublets couple separately to up- and down-type quarks. This is also of relevance for Supersymmetry, since this corresponds to the Higgs sector of any commonly used supersymmetric model. These models involve additional charged scalar particles, which contribute at tree level to the (semi)-leptonic B decays into a τ . The distinct feature of the 2HDMII is that the contributions of the charged scalars scale as $m_\tau^2/m_{H^\pm}^2$, since the couplings to the charged Higgs particles

are proportional to the mass of the lepton. As a consequence, one may expect visible effects in decays into a τ , but only small effects for decays into e and μ .

As discussed in the next section, the observations cannot be fitted to the expectations from the 2HDMII. To this end one has to extend the analysis to other models, where the scaling of the new contributions with the lepton mass is different.

Measurement of $\mathcal{R}_{D^{(*)}}$

The $\bar{B} \rightarrow D^{(*)}\tau\bar{\nu}_\ell$ decays have been studied at the $\Upsilon(4S)$ resonance, where the experimental signature consists of a D or D^* meson, an electron or muon from the decay $\tau \rightarrow \ell\nu_\tau\bar{\nu}_\ell$, a fully-reconstructed hadronic decay of the second B meson in the event and multiple missing neutrinos. The signal decays are separated from $\bar{B} \rightarrow D^{(*)}\ell\bar{\nu}_\ell$ decays using the measured missing mass squared; decays with only a single missing neutrino peak sharply at zero in this variable, while the signal is spread out to positive values. Background from $\bar{B} \rightarrow D^{**}\ell\bar{\nu}_\ell$ decays with one or more unreconstructed particles is harder to separate from signal.

Measurements from BELLE [147–149] and BABAR [150,146] have consistently resulted in values for \mathcal{R}_D and \mathcal{R}_{D^*} that exceed standard model predictions. The largest uncertainty is statistical; leading sources of systematic uncertainty include the modelling of semileptonic decays to charm final states with masses above m_{D^*} and the modelling of the selection efficiency for signal events. The first two BELLE measurements were untagged and are subject to larger systematic uncertainties. We choose to average the tagged measurements [149,146], and take the systematic uncertainties of the BELLE measurements to have a 50% correlation with each other and a 25% correlation with the BABAR measurements to find the values quoted in Eq. (40). If we include the untagged measurements (assuming 50%/25% correlation in systematic errors with other BELLE/BABAR measurements) we find $\mathcal{R}_D^{\text{meas}} = 0.427 \pm 0.060$ and $\mathcal{R}_{D^*}^{\text{meas}} = 0.345 \pm 0.028$. Some improvement should be possible with existing B-factory data sets.

Table 3 lists the inputs used in calculating the averages quoted here. Where the ratios $\mathcal{R}_{D^{(*)}}$ were not directly

measured, the branching fractions used to obtain these results were $\mathcal{B}(\overline{B}^0 \rightarrow D^{*+} \ell \overline{\nu}_\ell) = 0.0495 \pm 0.0011$ and $\mathcal{B}(\overline{B}^0 \rightarrow D^+ \ell \overline{\nu}_\ell) = 0.0213 \pm 0.0010$, with the corresponding B^- branching fractions obtained by multiplying by the lifetime ratio $\tau_{B^+}/\tau_{B^0} = 1.079 \pm 0.007$.

Table 3: Measurements of \mathcal{R}_D and \mathcal{R}_{D^*} times 10^2 .

		\mathcal{R}_D	\mathcal{R}_{D^*}
BABAR [146]	all B , tag	$44.0 \pm 5.8 \pm 4.2$	$33.2 \pm 2.4 \pm 1.8$
BELLE [149]	B^+ , tag	$70 \pm 19 \pm 10$	$47 \pm 11 \pm 7$
BELLE [149]	B^0 , tag	$48 \pm 21 \pm 6$	$48 \pm 13 \pm 5$
BELLE [147]	B^+ , no tag	$34 \pm 10 \pm 5$	$40 \pm 5 \pm 5$
BELLE [148]	B^0 , no tag		$41 \pm 8 \pm 7$

The tension between the SM prediction and the measurements at the level of 2.4σ and 3.0σ lead to various speculations on possible new physics contributions. It is striking that an interpretation in terms of the 2HDMII seems to be ruled out by the data. Fig. 2 shows that the interpretation of the deviation of \mathcal{R}_D in terms of the 2HDMII requires vastly different values of the relevant parameter $\tan\beta/m_{H^+}$ than for \mathcal{R}_{D^*} , excluding this possibility.

A more general approach has been formulated in [153] on the basis of an effective field theory consideration. Assuming lepton-flavour universality (LFU) violating operators of dimension six and eight the observed values can be fitted to the coefficients of these operators. Although a detailed analysis along these lines requires to have more data on related decays (such as $B \rightarrow \pi\tau\overline{\nu}$), there are indications that the tension in $\mathcal{R}_{D^{(*)}}$ cannot be explained by a minimally flavor-violating scenario with only left-handed interactions; a better fit is obtained once right-handed and scalar currents are involved.

Conclusion

The study of semileptonic B meson decays continues to be an active area for both theory and experiment. Substantial progress has been made in the application of HQE calculations

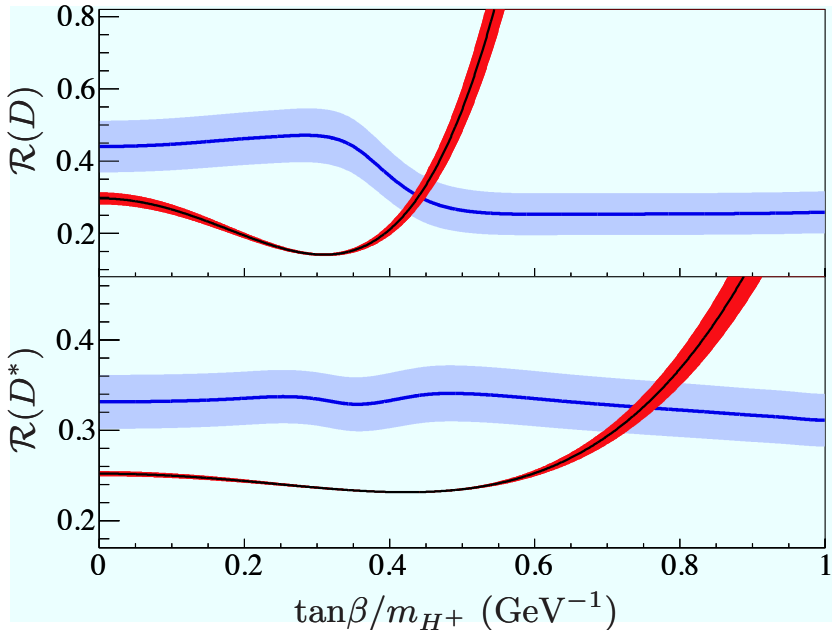


Figure 2: The $\mathcal{R}_{D^{(*)}}$ measured in Ref. 146 along with expectations in the 2HDMII as a function of $\tan\beta/m_{H^+}$.

to inclusive decays, where fits to moments of $\bar{B} \rightarrow X_c \ell \bar{\nu}_\ell$ decays provide precise values for $|V_{cb}|$ and, in conjunction with $B \rightarrow X_s \gamma$ decays or input on m_c , provide precise and consistent values for m_b . The values from the inclusive and exclusive $|V_{cb}|$ determinations are marginally consistent.

Continued improvements in measurements of inclusive $\bar{B} \rightarrow X_u \ell \bar{\nu}_\ell$ decays, along with additional theoretical studies of higher order contributions and improved knowledge of m_b , have strengthened our determination of $|V_{ub}|$. Further progress in this area is possible, but will require better theoretical control over higher order terms, and improved experimental knowledge of the $\bar{B} \rightarrow X_c \ell \bar{\nu}_\ell$ background.

Progress in both $b \rightarrow u$ and $b \rightarrow c$ exclusive channels depends crucially on progress in lattice QCD calculations. Here the prospects are good, since unquenched calculations are now available for the semileptonic form factors discussed here, as well as for other hadronic weak matrix elements needed to

obtain the elements and phase of the CKM matrix [156,157]. Projections for future uncertainties from lattice calculations can be found in Ref. 158.

The measurements of the $\overline{B} \rightarrow \pi \ell \overline{\nu}_\ell$ branching fraction have uncertainties below 4%, and the measured q^2 dependence is reasonably precise. Reducing the theoretical uncertainties to a comparable level will require significant effort, but is essential.

The tension between the values for $|V_{ub}|$ obtained from inclusive and exclusive decays has persisted for many years, despite significant improvements in both theory and experiment for both methods. How to reconcile these results remains an intriguing puzzle.

Both $|V_{cb}|$ and $|V_{ub}|$ are indispensable inputs into unitarity triangle fits. In particular, knowing $|V_{ub}|$ with good precision allows a test of CKM unitarity in the most direct way, by comparing the length of the $|V_{ub}|$ side of the unitarity triangle with the measurement of $\sin(2\beta)$. This comparison of a “tree” process ($b \rightarrow u$) with a “loop-induced” process ($B^0 - \overline{B}^0$ mixing) provides sensitivity to possible contributions from new physics.

The observation of semileptonic decays into τ leptons has opened a new window to the physics of the third generation. The data indicate a tension between the data and the standard model prediction, which could be a hint to new physics. However, the most prominent and simplest candidate, the 2HDMII, cannot explain the current data. More general ansätze can fit the data, but do not lead to a deeper insight unless measurements of related processes (such as $B \rightarrow \pi \tau \overline{\nu}$) are available.

The authors would like to acknowledge helpful input from F. Bernlochner, P. Gambino and C. Schwanda.

References

1. See R. Kowalewski and T. Mannel in Phys. Rev. **D86**, 010001 (2012).
2. Y. Amhis *et al.*, arXiv:1207.1158.
3. N. Isgur and M.B. Wise, Phys. Lett. **B232**, 113 (1989); *ibid.* **B237**, 527 (1990).
4. M.A. Shifman and M.B. Voloshin, Sov. J. Nucl. Phys. **47**, 511 (1988) [Yad. Fiz. **47**, 801 (1988)].
5. M.E. Luke, Phys. Lett. **B252**, 447 (1990).

6. M. Ademollo and R. Gatto, Phys. Rev. Lett. **13**, 264 (1964).
7. A.V. Manohar and M.B. Wise, Camb. Monogr. Part. Phys. Nucl. Phys. Cosmol. **10**,1(2000);
H. Georgi, Phys. Lett. **B240**, 447 (1990);
A.F. Falk *et al.*, Nucl. Phys. **B343**, 1 (1990);
E. Eichten and B. Hill, Phys. Lett. **B234**, 511 (1990).
8. A. Sirlin, Nucl. Phys. **B196**, 83 (1982).
9. C.G. Boyd, B. Grinstein, and R.F. Lebed, Phys. Rev. **D56**, 6895 (1997); *ibid.*, Phys. Rev. Lett. **74**, 4603 (1995);
C.G. Boyd and M.J. Savage, Phys. Rev. **D56**, 303 (1997).
10. I. Caprini *et al.*, Nucl. Phys. **B530**, 153 (1998).
11. A. Czarnecki and K. Melnikov, Nucl. Phys. **B505**, 65 (1997).
12. S. Hashimoto *et al.*, Phys. Rev. **D66**, 014503 (2002).
13. S. Hashimoto *et al.*, Phys. Rev. **D61**, 014502 (2000).
14. Jon A. Bailey *et al.*, Fermilab Lattice and MILC collaborations, *Proceedings of Science LATTICE2010* (2010) 311. This is an update of C. Bernard *et al.*, Phys. Rev. **D79**, 014506 (2009).
15. I.I.Y. Bigi *et al.*, Phys. Rev. **D52**, 196 (1995).
16. A. Kapustin *et al.*, Phys. Lett. B **375**, 327 (1996).
17. P. Gambino, T. Mannel, and N. Uraltsev, Phys. Rev. **D81**, 113002 (2010).
18. P. Gambino, T. Mannel and N. Uraltsev, JHEP **1210**, 169 (2012).
19. D. Buskulic *et al.*, (ALEPH Collab.), Phys. Lett. **B395**, 373 (1997).
20. G. Abbiendi *et al.*, (OPAL Collab.), Phys. Lett. **B482**, 15 (2000).
21. P. Abreu *et al.*, (DELPHI Collab.), Phys. Lett. **B510**, 55 (2001).
22. J. Abdallah *et al.*, (DELPHI Collab.), Eur. Phys. J. **C33**, 213 (2004).
23. N.E. Adam *et al.*, (CLEO Collab.), Phys. Rev. **D67**, 032001 (2003).
24. B. Aubert *et al.*, (BABAR Collab.), Phys. Rev. **D77**, 032002 (2008).
25. B. Aubert *et al.*, (BABAR Collab.), Phys. Rev. Lett. **100**, 231803 (2008).
26. B. Aubert *et al.*, (BABAR Collab.), Phys. Rev. **D79**, 012002 (2009).

27. W. Dungen *et al.*, (BELLE Collab.), Phys. Rev. **D82**, 112007 (2010).
28. See slac.stanford.edu/xorg/hfag/semi/ update to Ref. [2] for PDG 2013.
29. J. Beringer *et al.*(Particle Data Group), Phys. Rev. **D86**, 010001 (2012) and 2013 partial update for the 2014 edition.
30. N. Uraltsev, Phys. Lett. **B585**, 253 (2004).
31. M. Okamoto *et al.*, Nucl. Phys. (Proc. Supp.) **B140**, 461 (2005). A. Kronfeld, talk presented at the workshop CKM05, San Diego, CA - Workshop on the Unitarity Triangle, 15-18 March 2005.
32. B. Aubert *et al.*, (BABAR Collab.), Phys. Rev. Lett. **104**, 011802 (2010).
33. J. E. Bartelt *et al.*, (CLEO Collab.), Phys. Rev. Lett. **82**, 3746 (1999).
34. K. Abe *et al.*, (BELLE Collab.), Phys. Lett. **B526**, 247 (2002).
35. A.V. Manohar and M.B. Wise, Phys. Rev. **D49**, 1310 (1994).
36. I.I.Y. Bigi *et al.*, Phys. Rev. Lett. **71**, 496 (1993), Phys. Lett. **B323**, 408 (1994).
37. M.A. Shifman, I.I.Y. Bigi, and N. Uraltsev, Int. J. Mod. Phys. **A16**, 5201 (2001).
38. D. Benson *et al.*, Nucl. Phys. **B665**, 367 (2003).
39. M. Gremm and A. Kapustin, Phys. Rev. **D55**, 6924 (1997).
40. B. M. Dassinger, T. Mannel, and S. Turczyk, JHEP **0703**, 087 (2007).
41. I. I. Bigi, N. Uraltsev, and R. Zwicky, Eur. Phys. J. **C50**, 539 (2007).
42. T. Mannel, S. Turczyk, and N. Uraltsev, JHEP **1011**, 109 (2010).
43. A. Pak and A. Czarnecki, Phys. Rev. D **78**, 114015 (2008).
44. S. Biswas and K. Melnikov, JHEP **1002**, 089 (2010).
45. P. Gambino, JHEP **1109**, 055 (2011).
46. P. Gambino and N. Uraltsev, Eur. Phys. J. **C34**, 181 (2004).
47. V. Aquila *et al.*, Nucl. Phys. B **719**, 77 (2005).
48. T. Becher, H. Boos, and E. Lunghi, JHEP **0712**, 062 (2007).

49. A. Alberti *et al.*, Nucl. Phys. B **870**, 16 (2013).
50. C. Breidenbach *et al.*, Phys. Rev. D **78**, 014022 (2008).
51. I. Bigi *et al.*, JHEP **1004**, 073 (2010).
52. A.H. Hoang *et al.*, Phys. Rev. **D59**, 074017 (1999).
53. H. Leutwyler, Phys. Lett. **B98**, 447 (1981);
M.B. Voloshin, Sov. J. Nucl. Phys. **36**, 143 (1982).
54. A.H. Hoang, Phys. Rev. D **61**, 034005 (2000).
55. S.E. Csorna *et al.*, (CLEO Collab.), Phys. Rev. **D70**, 032002 (2004).
56. A.H. Mahmood *et al.*, (CLEO Collab.), Phys. Rev. **D70**, 032003 (2004).
57. B. Aubert *et al.*, (BABAR Collab.), Phys. Rev. **D69**, 111103 (2004).
58. B. Aubert *et al.*, (BABAR Collab.), Phys. Rev. **D69**, 111104 (2004).
59. C. Schwanda *et al.*, (BELLE Collab.), Phys. Rev. **D75**, 032005 (2007).
60. P. Urquijo *et al.*, (BELLE Collab.), Phys. Rev. **D75**, 032001 (2007).
61. J. Abdallah *et al.*, (DELPHI Collab.), Eur. Phys. J. **C45**, 35 (2006).
62. D. Acosta *et al.*, (CDF Collab.), Phys. Rev. **D71**, 051103 (2005).
63. B. Aubert *et al.*, (BABAR Collab.), Phys. Rev. **D81**, 032003 (2010).
64. A. Limosani *et al.* [BELLE Collab.], Phys. Rev. Lett. **103**, 241801 (2009).
65. C. Schwanda *et al.*, (BELLE Collab.), Phys. Rev. **D78**, 032016 (2008).
66. B. Aubert *et al.*, (BABAR Collab.), Phys. Rev. **D72**, 052004 (2005).
67. B. Aubert *et al.*, (BABAR Collab.), Phys. Rev. Lett. **97**, 171803 (2006).
68. S. Chen *et al.*, (CLEO Collab.), Phys. Rev. Lett. **87**, 251807 (2001).
69. M. Battaglia *et al.*, Phys. Lett. **B556**, 41 (2003).
70. B. Aubert *et al.*, (BABAR Collab.), Phys. Rev. Lett. **93**, 011803 (2004).
71. O. Buchmüller and H. Flächer, hep-ph/0507253; updated in Ref. 28.
72. C. W. Bauer *et al.*, Phys. Rev. **D70**, 094017 (2004); updated in Ref. 28.

73. See section 5.4.2 of M. Antonelli *et al.*, Phys. Reports **494**, 197 (2010).
74. B.Dehnadi, *et al.*, arXiv:1102.2264.
75. I. Allison *et al.*, (HPQCD Collab.), Phys. Rev. **D78**, 054513 (2008).
76. Chetyrkin *et al.*, Phys. Rev. **D80**, 074010 (2009).
77. P. Gambino and C. Schwanda, Phys. Rev. **D89**, 014022 (2014).
78. T. Ewerth, P. Gambino, and S. Nandi, Nucl. Phys. B **830**, 278 (2010).
79. A. H. Hoang *et al.*, Phys. Rev. **D59**, 074017 (1999).
80. N. Uraltsev, Int. J. Mod. Phys. **A14**, 4641 (1999).
81. M. Neubert, Phys. Rev. **D49**, 4623 (1994); *ibid.* **D49**, 3392 (1994).
82. I. Bigi *et al.*, Int. J. Mod. Phys. **A9**, 2467 (1994).
83. B.O. Lange, M. Neubert, and G. Paz, Phys. Rev. **D72**, 073006 (2005).
84. C. W. Bauer *et al.*, Phys. Lett. **B543**, 261 (2002).
85. T. Mannel and S. Recksiegel, Phys. Rev. **D60**, 114040 (1999).
86. C. W. Bauer, Z. Ligeti, and M. E. Luke, Phys. Rev. **D64**, 113004 (2001).
87. C. W. Bauer *et al.*, Phys. Rev. **D68**, 094001 (2003).
88. M. Neubert, Phys. Lett. **B513**, 88 (2001); Phys. Lett. **B543**, 269 (2002).
89. A.K. Leibovich *et al.*, Phys. Rev. **D61**, 053006 (2000); **62**, 014010 (2000); Phys. Lett. **B486**, 86 (2000); **513**, 83 (2001).
90. A.H. Hoang *et al.*, Phys. Rev. **D71**, 093007 (2005).
91. B. Lange *et al.*, JHEP **0510**, 084 (2005); B. Lange, JHEP **0601**, 104 (2006).
92. M. Neubert, Phys. Lett. **B612**, 13 (2005).
93. Z. Ligeti, I. W. Stewart, and F. J. Tackmann, Phys. Rev. D **78**, 114014 (2008).
94. P. Gambino *et al.*, JHEP **0710**, 058 (2007).
95. J.R. Andersen and E. Gardi, JHEP **0601**, 097 (2006).
96. C. Greub, M. Neubert, and B.D. Pecjak, Eur. Phys. J. **C65**, 501(2010).
97. M. Brucherseifer, F. Caola, and K. Melnikov, Phys. Lett. B **721**, 107 (2013).

98. C. W. Bauer *et al.*, Phys. Rev. **D64**, 113004 (2001); Phys. Lett. **B479**, 395 (2000).
99. I. I. Y. Bigi and N. G. Uraltsev, Nucl. Phys. **B423**, 33 (1994).
100. M.B. Voloshin, Phys. Lett. **B515**, 74 (2001).
101. Z. Ligeti, M. Luke, and A. V. Manohar, Phys. Rev. **D82**, 033003 (2010).
102. P. Gambino and J. F. Kamenik, Nucl. Phys. **B840**, 424 (2010).
103. J.L. Rosner *et al.*, (CLEO Collab.), Phys. Rev. Lett. **96**, 121801 (2006).
104. B. Aubert *et al.*, (BABAR Collab.), arXiv:0708.1753.
105. R. Barate *et al.*, (ALEPH Collab.), Eur. Phys. J. **C6**, 555 (1999).
106. M. Acciarri *et al.*, (L3 Collab.), Phys. Lett. **B436**, 174 (1998).
107. G. Abbiendi *et al.*, (OPAL Collab.), Eur. Phys. J. **C21**, 399 (2001).
108. P. Abreu *et al.*, (DELPHI Collab.), Phys. Lett. **B478**, 14 (2000).
109. A. Bornheim *et al.*, (CLEO Collab.), Phys. Rev. Lett. **88**, 231803 (2002).
110. A. Limosani *et al.*, (BELLE Collab.), Phys. Lett. **B621**, 28 (2005).
111. B. Aubert *et al.*, (BABAR Collab.), Phys. Rev. **D73**, 012006 (2006).
112. B. Aubert *et al.*, (BABAR Collab.), Phys. Rev. Lett. **95**, 111801 (2005), Erratum-*ibid.* **97**, 019903(E) (2006).
113. R. Kowalewski and S. Menke, Phys. Lett. **B541**, 29 (2002).
114. J. P. Lees *et al.*, (BABAR Collab.), arXiv:1112.0702.
115. I. Bizjak *et al.*, (BELLE Collab.), Phys. Rev. Lett. **95**, 241801 (2005).
116. P. Urquijo *et al.*, (BELLE Collab.), Phys. Rev. Lett. **104**, 021801 (2010).
117. V. Golubev, Y. Skovpen, and V. Luth, Phys. Rev. **D76**, 114003 (2007).
118. B. Aubert *et al.*, (BABAR Collab.), Phys. Rev. Lett. **96**, 221801 (2006).
119. H. Kakuno *et al.*, (BELLE Collab.), Phys. Rev. Lett. **92**, 101801 (2004).

120. A. Sibidanov *et al.*, (BELLE Collab.), Phys. Rev. **D88**, 032005 (2013).
121. B. Aubert *et al.*, (BABAR Collab.), Phys. Rev. Lett. **90**, 181801 (2003).
122. T. Hokuue *et al.*, (BELLE Collab.), Phys. Lett. **B648**, 139 (2007).
123. B. Aubert *et al.*, (BABAR Collab.), Phys. Rev. **D79**, 052011 (2008).
124. C. Schwanda *et al.*, (BELLE Collab.), Phys. Rev. Lett. **93**, 131803 (2004).
125. N. E. Adam *et al.*, (CLEO Collab.), Phys. Rev. Lett. **99**, 041802 (2007); Phys. Rev. **D76**, 012007 (2007); supercedes Phys. Rev. **D68**, 072003 (2003).
126. P. del Amo Sanchez *et al.*, (BABAR Collab.), Phys. Rev. **D83**, 032007 (2011); supercedes B. Aubert *et al.*, (BABAR Collab.), Phys. Rev. **D72**, 051102 (2005).
127. P. del Amo Sanchez *et al.*, (BABAR Collab.), Phys. Rev. **D83**, 052011 (2011); updated in J. P. Lees *et al.*, (BABAR Collab.), Phys. Rev. **D86**, 092004 (2012).
128. J. Bailey *et al.*, (Fermilab/MILC), Phys. Rev. **D79**, 054507 (2009).
129. E. Dalgic *et al.*, (HPQCD), Phys. Rev. **D73**, 074502 (2006), Erratum-*ibid.* **D75** 119906 (2007).
130. T. Becher and R. J. Hill, Phys. Lett. **B633**, 61 (2006).
131. M. C. Arnesen *et al.*, Phys. Rev. Lett. **95**, 071802 (2005).
132. T. Hurth *et al.*, hep-ph/0509167.
133. M.A. Shifman, A.I. Vainshtein, and V.I. Zakharov, Nucl. Phys. **B147**, 385 (1979); *ibid.* **B147**, 448 (1979).
134. P. Ball and R. Zwicky, Phys. Rev. **D71**, 014015 (2005).
135. G. Duplancic *et al.*, JHEP **0804**, 014 (2008).
136. A. Khodjamirian *et al.*, Phys. Rev. **D83**, 094031 (2011).
137. A. Bharucha, JHEP **1205**, 092 (2012).
138. C. Bourrely, I. Caprini, and L. Lellouch, Phys. Rev. **D79**, 013008 (2009).
139. H. Ha *et al.*, (BELLE Collab.), Phys. Rev. **D83**, 071101 (2011).
140. K. Abe *et al.*, (BELLE Collab.), Phys. Lett. **B648**, 139 (2007).
141. B. Aubert *et al.*, (BABAR Collab.), Phys. Rev. Lett. **101**, 081801 (2008).
142. B. Aubert *et al.*, (BABAR Collab.), Phys. Rev. Lett. **97**, 211801 (2006).

143. W. Brower and H. Paar, Nucl. Instrum. Methods **A421**, 411 (1999).
144. P. Ball, [arXiv:0705.2290](https://arxiv.org/abs/0705.2290);
J.M. Flynn and J. Nieves, Phys. Lett. **B649**, 269 (2007);
T. Becher and R.J. Hill, Phys. Lett. **B633**, 61 (2006);
M. Arnesen *et al.*, Phys. Rev. Lett. **95**, 071802 (2005).
145. M. Tanaka, Z. Phys. **C67**, 321 (1995);
H. Itoh, S. Komine, and Y. Okada, Prog. Theor. Phys. **114**, 179 (2005);
U. Nierste, S. Trine, and S. Westhoff, Phys. Rev. **D78**, 015006 (2008);
M. Tanaka and R. Watanabe, Phys. Rev. **D82**, 034027 (2010);
S. Fajfer, J. F. Kamenik, and I. Nišandžić, Phys. Rev. **D85**, 094025 (2012).
146. J. Lees *et al.*, (Babar Collab.), Phys. Rev. Lett. **109**, 101802 (2012).
147. A. Bozek *et al.*, (Belle Collab.), Phys. Rev. **D82**, 072005 (2010).
148. A. Matyja *et al.*, (Belle Collab.), Phys. Rev. Lett. **99**, 191807 (2007).
149. I. Adachi *et al.*, (Belle Collab.), [arXiv:0910.430](https://arxiv.org/abs/0910.430).
150. B. Aubert *et al.*, (Babar Collab.), Phys. Rev. Lett. **100**, 021801 (2008).
151. A. Datta, M. Duraisamy, and D. Ghosh, Phys. Rev. **D86**, 034027 (2012).
152. D. Becirevic, N. Kosnik, and A. Tayduganov, Phys. Lett. **B716**, 208 (2012).
153. S. Fajfer *et al.*, Phys. Rev. Lett. **109**, 161801 (2012).
154. A. Crivellin, C. Greub, and A. Kokulu, Phys. Rev. **D86**, 054014 (2012).
155. J. G. Körner and G. A. Schuler, Z. Phys. **C46**, 93 (1990).
156. J. Laiho, E. Lunghi, and R. S. Van de Water, Phys. Rev. **D 81**, 034503 (2010).
157. G. Colangelo, *et al.*, Eur. Phys. J. C **71**, 1695 (2011).
158. USQCD Collab. (2011),
www.usqcd.org/documents/HiIntensityFlavor.pdf.